Journal of Metals, Materials and Minerals, Vol. 29, No. 4, pp. 90-98, 2019

Reducing water absorption of fiber-cement composites for exterior applications by crystal modification method

Parinya CHAKARTNARODOM[1], Nuntaporn KONGKAJUN[2,*], Nutthita CHUANKRERKKUL[3], Pitcharat INEURE[4], and Wichit PRAKAYPAN[5]

[1] *Department of Materials Engineering, Faculty of Engineering, Kasetsart University, Chatuchak, Bangkok, 10900, Thailand*
[2] *Department of Materials and Textile Technology, Faculty of Science and Technology, Thammasat University, Klong Luang, Prathumthani, 12121, Thailand*
[3] *Metallurgy and Materials Science Research Institute, Chulalongkorn University, Patumwan, Bangkok, 10330, Thailand*
[4] *Glass Bridge Company Limited, Wang Thonglang, Bangkok, 10310, Thailand*
[5] *Shera Public Company Limited, Bangkorlhaem, Bangkok, 10120, Thailand*

[*]**Corresponding author e-mail:** n-kongkj@tu.ac.th

Received date:
30 September 2018
Revised date:
18 March 2019
Accepted date:
23 March 2019

Keywords:
Crystal modification
Fiber-cement composites
Fiber-cement products
Water absorption
Exterior applications

Abstract

The aim of this work was to reduce the water absorption of the fiber-cement composites, which is also known as fiber-cement products, by the crystal modification of cement matrix using the additives including polyurethane-based corn starch–lithium perchlorate ($LiClO_4$), and acrylic resin emulsion-based chitosan-silicate hybrid compound. To prepare the samples, the mixtures consisting Portland cement Type I, sand, cellulose fibers from pine trees, gypsum, and additive were mixed with water. The percentages of additive in the mixtures before mixing with water were 0.03 to 0.17 wt%. The green sheets of samples were formed by filter-pressing method, air cured for 1 day, and then autoclaved at 8 bars and 140°C for 12 h. The experimental results indicated that the water absorption of the samples was reduced when polyurethane-based corn starch–lithium perchlorate ($LiClO_4$) was used as the additive due to the crystallization of the small crystals within cement matrix, while their mechanical properties including modulus of rupture (MOR) and modulus of elasticity (MOE) of the samples using this additive conform industrial standard.

1. Introduction

Fiber-cement composites are the ceramic-matrix composite building materials in which the cement matrix is reinforced with the fibers such as cellulose fibers and synthetic fibers. For exterior applications such as flooring, roofing, and wall applications (Figure 1), fiber-cement composites will expose to the aggressive environments such as frequent weather change, high relative humidity, and acid rain. Therefore, beside the strength, water absorption is another important physical property for the fiber-cement composites. In the industry, fiber-cement composites for exterior applications are typically coated with the chemicals in order to reduce their water absorption. However, the performance of the coating could be deteriorated overtime during their service.

Generally, the raw materials for manufacturing the fiber-cement composites are Portland cement, silica sand, fibers, additives, and water. These raw materials are mixed and molded into the green sheets by a process such as filter pressing, Hatschek process, Magnani process, injection molding, extrusion, mold casting, flow-on process, and roll forming [2-4]. Regularly, the additives are used in fiber-cement composites for reducing the amount of water for the forming process and/or improving the properties of the finished products.

Due to the growing environmental concerns, the using of natural organic materials as the additive for cement and concrete gain more interest from the scientists and the construction materials industry. Chitosan is a biopolymer derived from chitin, a natural-occurring material that could be obtained from the shell of the crustaceans and the insects. Chitosan has wide area of applications because of its properties such as biocompatibility, biodegrability, anti-bacterial activity, and non-toxicity. Examples of chitosan's applications are biological adhesive, biosensors, food packaging, and water treatment. [5-6] For the applications of chitosan in cement-based materials, it was found that when using chitosan as a cement additive, chitosan could increase the viscosity of the cement mortar [7], improve the strength of the calcium phosphate cement [8] and the concrete [9]0, and reduce the total pores volume of the concrete [10]. Starch is another natural-occurring material which is widely available, relatively low cost, and biodegradable. Starch may be used as a source for thermoplastic production [11-12]. In electronic applications, there are the starch-based solid polymer

DOI: 10.14456/jmmm.2019.51

electrolytes. [13] For the applications for cement-based materials, according to Akindahunsi et al [14-15], the strength of the concrete was improved when starch was added.

Figure 1. Examples of the outdoor applications of fiber-cement composites (a) floor (b) roof and (c) wall [1]

Typically, after forming process, the green sheets of fiber-cement composites are cured under hydrothermal condition using the autoclave. Tobermorite is a crystalline phase of calcium silicate hydrate formed under hydrothermal condition in $CaO–SiO_2–H_2O$ system. [16] Typically, tobermorite is found in the autoclaved fiber-cement composites. According to Dachowski and Stępień [17], and Dachowski and Komisarczyk [18], it was found that using the lithium compound such as lithium silicate as the additive in the lime-sand mixture for producing autoclaved silicate products affected their microstructure and improved both the water absorption and the compressive strength of the products.

As mentioned before, beside the strength, water absorption is another important property of fiber-cement composites. Therefore, the aim of this work was to reduce the water absorption of the fiber-cement composites by using the additives including polyurethane-based corn starch–lithium perchlorate ($LiClO_4$), and acrylic resin emulsion-based chitosan-silicate hybrid compound. The correlation between the improved water absorption property and the effect of those additives on the crystal modification of cement matrix was observed by scanning electron microscope (SEM).

2. Experimental

2.1 Sample preparation

The raw materials for preparing the samples were Portland cement Type I, sand, gypsum, cellulose fibers from pine trees, and additives. The additives used in this work were
Additive A: Polyurethane-based corn starch–lithium perchlorate ($LiClO_4$), and
Additive B: Acrylic resin emulsion-based chitosan-silicate hybrid compound.

These raw materials were obtained from Shera Public Company Limited. Both additive A and B were developed under the licensing of Shera Pubic Company Limited.

Table 1 lists the compositions of the mixtures for the sample preparation. The dosages of additives were 0.03-0.17 wt%. Formula F0 was the control formula. It was a common formula of the fiber-cement composites used for outdoor applications. The mixtures were mixed with the water to form a slurry and then molded by filter pressing method. After that, the molded samples were air cured for 1 day and autoclaved at 140°C and 8 bars for 12 h.

Table 1. Formulations for sample preparation.

Materials	**Composition (wt%)**					
	F0	**F1**	**F2**	**F3**	**F4**	**F5**
Portland cement	34.00	34.00	34.00	34.00	34.00	34.00
Sand	34.00	34.00	34.00	34.00	34.00	34.00
Gypsum	26.20	26.17	26.15	26.10	26.06	26.03
Cellulose fibers	5.80	5.80	5.80	5.80	5.80	5.80
Additive (A or B)	0	0.03	0.05	0.10	0.14	0.17

2.2 Raw materials and sample characterization

The chemical composition of the raw materials including Portland cement Type I, sand, and gypsum were determined using x-ray fluorescence (XRF) spectrometer. The model of the XRF spectrometer was Panalytical-Minipal 4. Furthermore, the particle size of both sand and gypsum were analyzed by laser particle size analyzer. The model of laser particle size analyzer was Sympatec-HELOS/BR-multirange with QUIXEL dispersing unit.

Archimedes' method was used to characterize the samples after being autoclaved for their water absorption (WA), apparent porosity (AP), and bulk density (B).

$$\mathrm{WA} = \frac{\mathrm{W_w - W_d}}{\mathrm{W_d}} \times 100 \qquad (1)$$

$$\mathrm{AP} = \frac{\mathrm{W_w - W_d}}{\mathrm{W_w - W_s}} \times 100 \qquad (2)$$

$$\mathrm{B} = \frac{\mathrm{W_d}}{\mathrm{W_w - W_s}} \qquad (3)$$

where W_d is the weight of the dry sample, W_S is the weight of the sample suspended in water, and W_W is the weight of the sample after it was removed from water [19-20]. In this work, the samples were dried at 100°C for 24 h, then W_d was measured. After that, the samples were soaked in the water for 24 h, then W_S and W_W were measured.

Moreover, the mechanical properties including modulus of rupture (MOR) and modulus of elasticity (MOE) of the samples were obtained by bending test using universal testing machine (UTM) [20]. The model of UTM was Instron 3300 series. For each formula, 8 samples were used for each test. Prior to the mechanical testing, all samples were saturated with water by being soaked in the water for 24 h.

2.3 Statistical analysis

The statistical hypothesis test was utilized in order to

a) test the correlation between the amount of the added additive and the properties of the sample, and

b) comparing the performance of each additive based on the properties of the samples

For correlation analysis, the analysis of variance was used and the significant level (α) for the hypothesis test was 0.05. According to Walpole et al [21] for the case of polynomial regression model, $\mathrm{Y} = \beta_0 + \beta_1 \mathrm{x} + \beta_2 \mathrm{x}^2$, the equation is constructed by fitting the model with the data points $\{(\mathrm{x_i}, \mathrm{y_i}),\ \mathrm{i} = 1,2,\ldots\mathrm{n} \text{ and } \mathrm{n} > 2\}$. The quality of the fitted model can be tested by the analysis of variance. Table 2 lists the equations used for statistical hypothesis test. The null hypothesis (Ho) is rejected, if the value of test statistic f is greater than the critical value $\mathrm{f}_{\alpha=0.05}(\mathrm{v_1}, \mathrm{v_2})$ from the table of critical values of the F-distribution [21].

For the performance comparison of additives, the method of t- test for mean comparison was used. Similar to the previous test, the significant level (α) for the hypothesis test was 0.05. If the absolute value of test statistic t is greater than the absolute value of the critical value $t_{\alpha/2}$ from the table of critical values of the t-distribution, $|t| > |t_{\alpha/2}|$, the null hypothesis (H_o) is rejected [21].

The details on the statistical hypothesis test for the correlation analysis, and mean comparison can be found in Walpole et al [21].

3. Results and discussion

The chemical composition from XRF analysis of Portland cement type I, gypsum, and sand were shown in Table 4. Moreover, Figure 2 showed the results from laser particle size analyzer on the particle size distribution of gypsum and sand. The average particle size of gypsum and sand were 51.81 μm and 24.62 μm, respectively.

Table 2. Statistical hypothesis test for the polynomial correlation between x and y. Ho and H_1 are the null and alternative hypotheses. $\bar{y}$ is the average of y_i which is $\bar{y} = \frac{\sum_{i=0}^{n} \hat{y}_i}{n}$. $\hat{y}_i$ is the predicted value of y_i from the polynomial regression model. f is the test statistic. [21]

H_0	H_1	Degree of freedom (ν)	Test statistic
$\beta_1 = \beta_2 = 0$	Either $\beta_1 \neq 0$ or $\beta_2 \neq 0$	$\nu_1 = 2$ and $\nu_2 = (n-3)$	$f = \left(\frac{n-3}{2}\right)\frac{\sum_{i=1}^{n}(\hat{y}_i - \bar{y})^2}{\sum_{i=1}^{n}(y_i - \hat{y}_i)^2}$

Table 3. Statistical hypothesis test for mean comparison between two set of data. For data set i, μ_i and $\overline{X}_i$ are the population and sample mean, s_i and s_i^2 are the standard deviation and variance of the data of sample, and t is the test statistic. [21]

H_0	H_1	Degree of freedom (ν)	Test statistic
$\mu_1 = \mu_2$	$\mu_1 \neq \mu_2$	$\nu = \frac{\left((s_1^2/n_1) + (s_2^2/n_2)\right)^2}{\frac{(s_1^2/n_1)^2}{n_1 - 1} + \frac{(s_2^2/n_2)^2}{n_2 - 1}}$	$t = \frac{\bar{x}_1 - \bar{x}_2}{\sqrt{(s_1^2/n_1) + (s_2^2/n_2)}}$

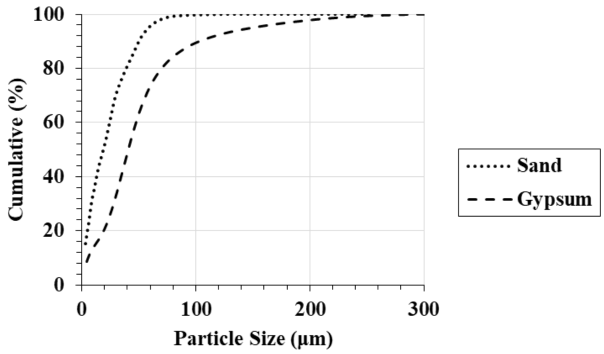

Figure 2. Cumulative particle size distribution of sand and gypsum

Figure 3 to Figure 7 showed the variation of properties of the samples with the change in dosage of additive A and additive B from 0.03 wt%. to 0.17 wt%. Even though the data on the properties of the samples can be fitted to the polynomial equations, the value of the test statistic f from Table 5 for all cases were lower than the critical value $f_{\alpha=0.05}(2,2) = 19.00$. Therefore, based on the statistical analysis, increasing the dosage of both additive A and additive B from 0.03 wt% (Formula F1) to 0.17 wt% (Formula F5) did not significantly affect the water absorption, apparent porosity, bulk density, MOR, and MOE of the samples.

Table 4 Chemical composition of Portland cement type I, gypsum, and sand

Composition (wt%)	**Portland cement type I**	**Gypsum**	**Sand**
CaO	62.23	24.56	0.15
SiO_2	19.34	0.139	95.41
Al_2O_3	5.81	0.15	2.12
Fe_2O_3	3.15	0.104	1.01
SO_3	2.65	73.07	0.12
MgO	1.25	0.198	0
K_2O	0.35	0.049	0.245
TiO_2	0.27	0.008	0.182
P_2O_5	0.09	0.344	0
Others	4.86	1.378	0.763

Table 5. Statistical hypothesis test for the polynomial correlation between the composition of the additive and the properties of the samples. (Figure 3 to Figure 7).

H_0	$\beta_1 = \beta_2 = 0$ No correlation between the dosage of additive and the observed property	
H_1	Either $\beta_1 \neq 0$ or $\beta_2 \neq 0$ There was the correlation between the dosage of additive and the observed property	
Critical value	$f_{\alpha=0.05}(2,2) = 19.00$	
Property	Value of test statistic (f)	
	Additive A	Additive B
Water absorption	1.30	2.80
Apparent porosity	0.96	10.88
Bulk density	2.03	0.84
MOR	1.71	1.33
MOE	7.32	7.30

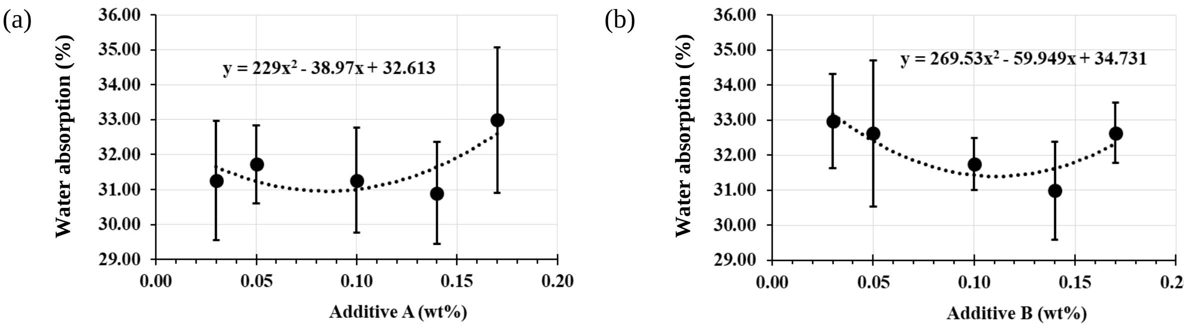

Figure 3. Water absorption of the samples (a) additive A (b) additive B.

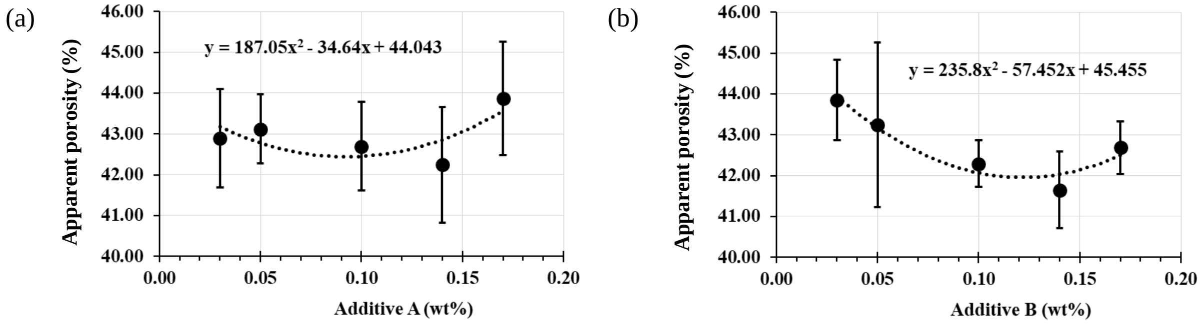

Figure 4. Apparent porosity of the samples (a) additive A (b) additive B.

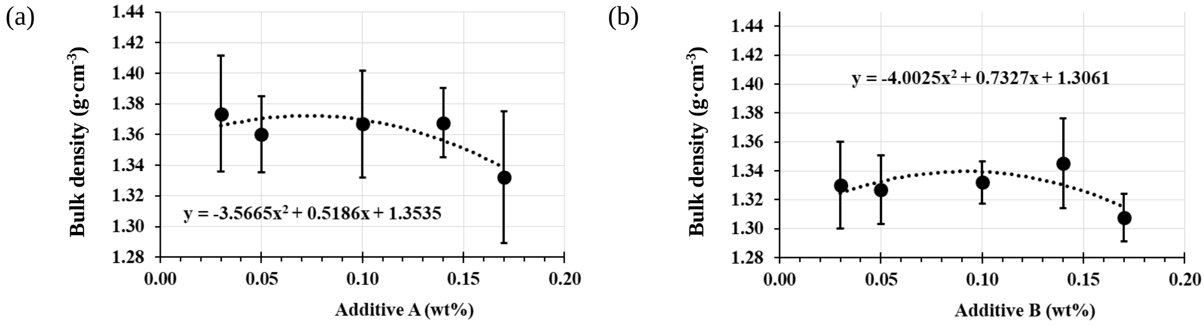

Figure 5. Bulk density of the samples (a) additive A (b) additive B

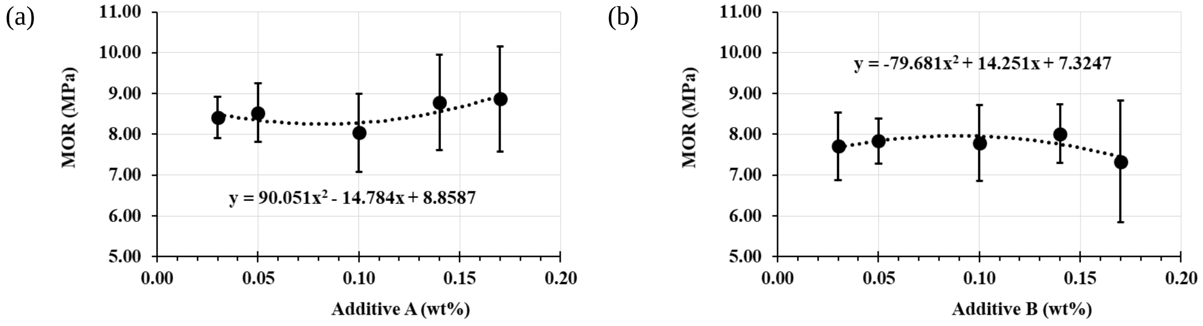

Figure 6. MOR of the samples (a) additive A (b) additive B.

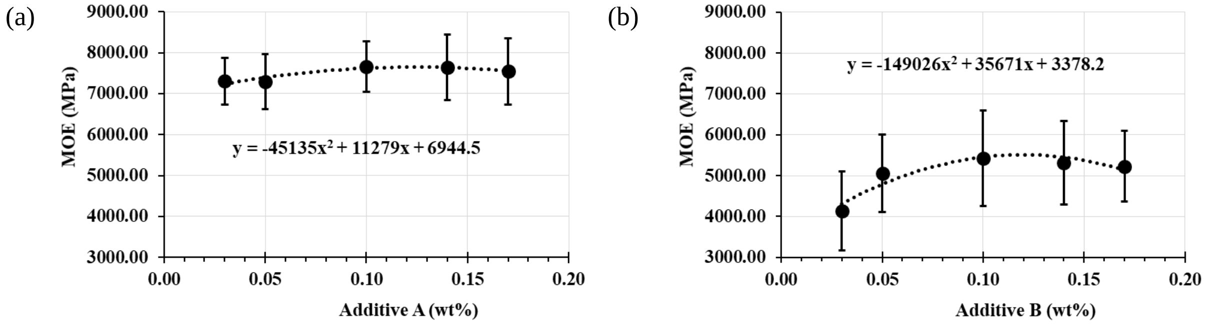

Figure 7. MOE of the samples (a) additive A (b) additive B.

Table 6 and Table 7 showed the results of statistical hypothesis test for the mean comparison of various properties between mean properties of the samples from Formula F0 (control formula) and mean properties of the samples from Formula F1 to F5.

For additive A, from Table 6, except MOR, the absolute values of test statistic ($|t|$) were greater than the absolute values of critical values ($|t_{\alpha/2}|$). Therefore, compared to the formula F0, for physical properties, using additive A could significantly reduce the water absorption, reduce the apparent porosity, and increase the bulk density of the samples. For mechanical properties, by using additive A, MOE of the samples was improved while MOR remained unchanged.

For additive B, from Table 7, except the bulk density, the absolute values of test statistic ($|t|$) were greater than the absolute values of critical values ($|t_{\alpha/2}|$). Therefore, compared to the formula F0, using additive B could significantly reduce the water absorption, reduce the apparent porosity, but did not significantly affect the bulk density of the samples. However, for mechanical properties, both MOR and MOE of the samples that employed additive B were lower.

Figure 8 to Figure 10 showed the SEM micrographs of the microstructures of the cement matrix of the samples with or without the using of additive. The crystalline phase shown on Figure 8 was tobermorite. Obviously, from Figure 9 and Figure 10, using the additives changed the morphology of the crystalline phase.

According to Meyers and Chawla [22], for the composite materials, both the microstructure of matrix phase and the interfacial interaction between matrix and reinforcement phase could affect the mechanical properties of the composite materials. Therefore, the change in morphology of the crystalline phase in cement matrix by using either additive A or B reduced the degree of water absorption and apparent porosity of the composites. Especially, for additive A, using this additive caused the nucleation of the small crystals which resulted in the improved packing efficiency of the crystalline phase. Then, this improved packing efficiency not only improved the physical properties (water absorption, apparent porosity, and bulk density) but also caused the improvement of MOE in the samples that used additive A.

Figure 11 showed the image of the actual fiber-cement board produced on the industrial scale at the factory of Shera Public Company Limited, Lop Buri, Thailand. Additive A was used in this case. Obviously, even though the surface of the fiber-cement board was cut, the water did not wet the slit.

Table 6. Statistical hypothesis test for mean comparison between the properties of the control formula (Formula F0) and the properties of the samples when Additive A was employed. For each property of samples that utilized additive A, the mean and the standard deviation were calculated from the data of all dosages of additive A (0.03-0.17 wt%).

H_0	$\mu_1 = \mu_2$ (Using the additive did not affected the observed property)					
H_1	$\mu_1 \neq \mu_2$					
Property	Formula F0		Formula F1 to F5		$\lvert t_{\alpha/2}\rvert$	$\lvert t\rvert$
	Mean	Variance	Mean	Variance		
Water absorption (%)	33.55	3.57	31.63	2.85	2.06	3.54
Apparent porosity (%)	44.40	1.92	42.96	1.61	2.06	3.58
Bulk density ($g\cdot cm^{-3}$)	1.33	1.39×10^{-3}	1.36	1.23×10^{-3}	2.06	3.22
MOR (MPa)	8.96	2.08	8.52	0.94	2.08	1.11
MOE (MPa)	5946	2.02×10^{6}	7374	0.48×10^{6}	2.11	3.71

Table 7. Statistical hypothesis test for mean comparison between the properties of the control formula (Formula F0) and the properties of the samples when Additive B was employed. For each property of the samples that utilized additive B, the mean and the standard deviation were calculated from the data of all dosages of additive B (0.03-0.17 wt%).

H_0	$\mu_1 = \mu_2$ (Using the additive did not affected the observed property)					
H_1	$\mu_1 \neq \mu_2$					
Property	Formula F0		Formula F1 to F5		$\lvert t_{\alpha/2}\rvert$	$\lvert t\rvert$
	Mean	Variance	Mean	Variance		
Water absorption (%)	33.55	3.57	32.15	2.20	2.07	2.63
Apparent porosity (%)	44.40	1.92	42.69	1.76	2.05	4.20
Bulk density ($g\cdot cm^{-3}$)	1.33	1.39×10^{-3}	1.33	0.62×10^{-3}	2.08	0.33
MOR (MPa)	8.96	2.08	7.73	0.88	2.09	3.15
MOE (MPa)	5946	2.02×10^{6}	5029	1.12×10^{6}	2.09	2.27

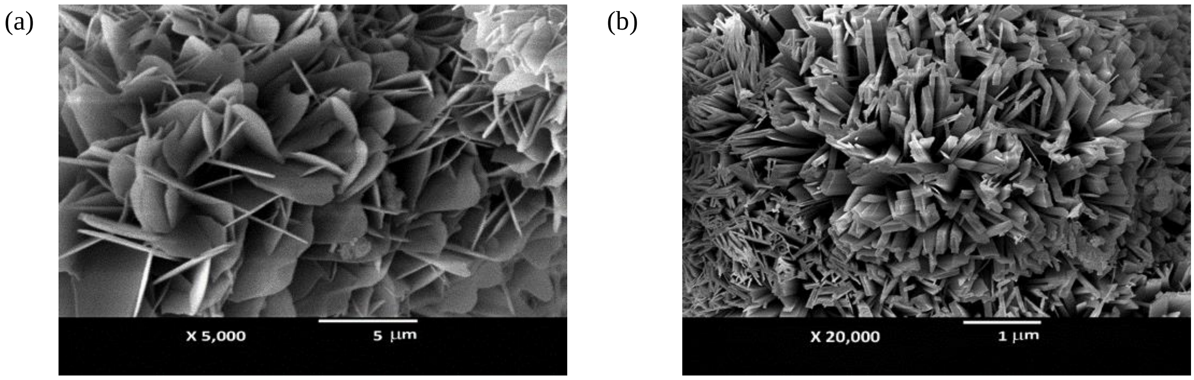

Figure 8. SEM micrographs showing the microstructure of the sample without using the additive.

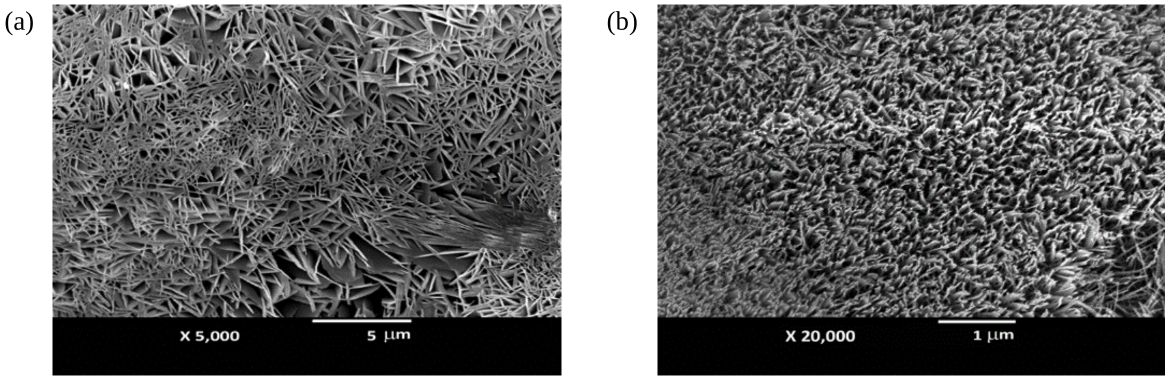

Figure 9. SEM micrographs showing the microstructure of the sample that used Additive A.

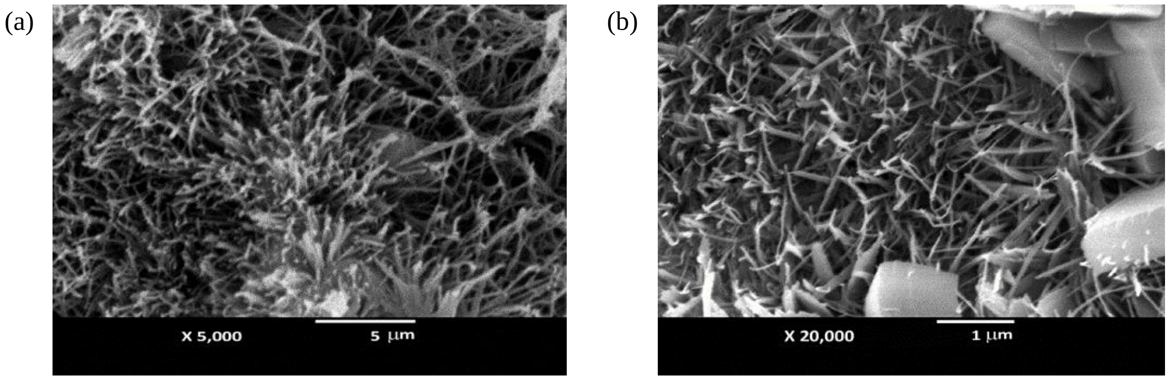

Figure 10. SEM micrographs showing the microstructure of the sample that used Additive B.

Figure 11. The actual fiber-cement board that used polyurethane-based corn starch–lithium perchlorate ($LiClO_4$) as the additive.

4. Conclusions

The aim of this work was to reduce the water absorption of the fiber-cement composites by using the additives including polyurethane-based corn starch–lithium perchlorate ($LiClO_4$) and acrylic resin emulsion-based chitosan-silicate hybrid compound. The results showed that

- Both compounds could be used for reducing the degree of water absorption in the fiber-cement composites.
- For mechanical properties, when polyurethane-based corn starch–lithium perchlorate ($LiClO_4$) was utilized, modulus of elasticity (MOE) of the samples was improved while modulus of rupture (MOR) remained unchanged.
- Increasing the amount of both additives in the samples from 0.03 wt% to 0.17 wt% did not significantly change the water absorption, apparent porosity, bulk density, MOR, and MOE of the samples.

5. Acknowledgements

This work was supported by Shera Public Company Limited.

References

[1] Shera Public Company Limited (2018), Project Reference. [image] Available at: https://www.Shera.com/th-en/project-reference [Accessed September 2018].

[2] P. Chakartnarodom, W. Prakaypan, P. Ineure, N. Kongkajun, and N. Chuankrerkkul, “Feasibility study of using basalt fibers as the reinforcement phase in fiber-cement products,” *Key Engineering Materials*, vol. 766, pp. 252-257, 2018

[3] S. Delvasto, E. F. Toro, F. Perdomo, and R. Mejía de Gutiérrez, “An appropriate vacuum technology for manufacture of corrugated fique fiber reinforced cementitious sheets,” *Construction and Building Materials*, vol. 24, pp. 187-192, 2010

[4] P. Chakartnarodom, W. Prakaypan, P. Ineure, N. Kongkajun, and N. Chuankrerkkul, “Formula of basalt fiber-reinforced cement board,” Thailand patent No.12440. Bangkok: Department of Intellectual Property, 2017

[5] C. Pandis, S. Madeira, J. Matos, A. Kyritsis, J. F. Mano, and J. L. G. Ribelles, “Chitosan–silica hybrid porous membranes,” *Materials Science and Engineering: C*, vol. 42, pp. 553-561, 2014

[6] H. Honarkar and M. Barikani, “Applications of biopolymers I: chitosan,” *Monatshefte für Chemie-Chemical Monthly*, vol. 140, pp. 1403, 2009

[7] M. Lasheras-Zubiate, I. Navarro-Blasco, J. M. Fernández, and J. I. Alvarez, “Studies on chitosan as an admixture for cement-based materials: Assessment of its viscosity enhancing effect and complexing ability for heavy metals,” *Journal of Applied Polymer Science*, vol. 120, pp. 242-252, 2011

[8] A. Aryaei, J. Liu, A. H. Jayatissa, and J. A. Champa, “Cross-linked chitosan improves the mechanical properties of calcium phosphate–chitosan cement,” *Materials Science and Engineering: C*, vol. 54, pp. 14-19, 2015

[9] U. T. Bezerra, R. M. Ferreira, and J. P. Castro-Gomes, “The effect of latex and chitosan biopolymer on concrete properties and performance,” *Key Engineering Materials*, vol. 466, pp. 37-46, 2011

[10] Y. V. Ustinova and T. P. Nikiforova, “Cement compositions with the chitosan additive,” *Procedia Engineering*, vol. 153, pp. 810-815, 2016

[11] J. F. A. Carvalho, “7 - Starch: Major Sources, Properties and Applications as thermoplastic materials,” in *Handbook of biopolymers and biodegradable plastics*, ed. S. Ebnesajjad: William Andrew Publishing, 2013, pp. 129-152

[12] X. S. Sun, “11 - Plastics derived from starch and poly (lactic acids),” in *Bio-Based Polymers and Composites*, eds R. P. Wool and X. S. Sun: Academic Press, 2005, pp. 369-410

[13] K. H. Teoh, S. Ramesh, and A. K. Arof, “Investigation on the effect of nanosilica towards corn starch–lithium perchlorate-based polymer electrolytes,” *Journal of Solid State Electrochemistry*, vol 16, pp. 3165-3170, 2012

[14] A. Akindahunsi, H. C. Uzoegbo, and S. Iyuke, “Use of starch modified concrete as a repair material,” in *3rd International Conference on Repair, Rehabilitation and Retrofitting*: Taylor & Francis Group, 2012, pp. 938-943

[15] A. Akindahunsi, W. Schmidt, H. C. Uzoegbo, and S. Iyuke, “The influence of starches on some properties of concrete,” in *International Conference on Advances in Cement and Concrete Technology in Africa*, eds. H. C. Uzoegbo and W. Schmidt, pp. 637-645, 2013

[16] L. Galvánková, J. Másilko, T. Solný, and E. Štěpánková, “Tobermorite synthesis under hydrothermal conditions,” *Procedia Engineering*, vol. 151, pp. 100-107, 2016

[17] R. Dachowski and A. Stępień, “The impact of various additives on the microstructure of silicate products,” *Procedia Engineering*, vol. 21, pp. 1173-1178, 2011.

[18] R. Dachowski and K. Komisarczyk, “Determination of microstructure and phase composition of sand-lime brick after autoclaving process,” *Procedia Engineering*, vol. 161, pp. 747-753, 2016

[19] D. R. Askeland, P. P. Fulay, and W. J. Wright, *The science and engineering of materials*. KY: CL Engineering, 2010

[20] ASTM C1185, "Standard test methods for sampling and testing non-asbestos fiber-cement flat sheet, roofing and siding shingles, and clapboards," ASTM International, West Conshohocken, PA.

[21] R. E. Walpole, R. H. Myers, S. L. Myers, and K. Ye, *Probability and Statistics for Engineers and Scientists*. New Jersey: Pearson, 2012.

[22] M. A. Meyers and K. K. Chawla, *Mechanical Behavior of Materials*, Prentice-Hall, Inc., 1999.